Transient Rheological Behavior of Semisolid SEED-Processed 7075 Aluminum Alloys in Rapid Compression

AMIR BOLOURI and X.-GRANT CHEN

The transient rheological behavior and microstructure evolution of semisolid SEED-processed 7075 aluminum alloys were studied using the rapid compression tests. The effects of the TiB_2 grain refinement on the grain morphology and size of semisolid slurries were investigated. Results indicated that the grain refiner could reduce the grain size and improve the globularity of α-Al grains. The grain-refined alloy can be easily deformed at a wide range of solid contents (0.42 to 0.53 Fs), in which the deformation level appears to be independent from the solid content. Under the transient state, the apparent viscosity decreased with increasing shear rate to a minimum value and followed by an increase as the shear rate decreased. The apparent viscosity of the base alloy exhibited a dependency on the solid content, while the apparent viscosity of the grain-refined alloy in the decreasing or increasing shear rate periods was not substantially influenced by the solid content. The viscosity as a function of applied shear rate can be described using the power law viscosity model. The differences in the flow behavior index (n) and the consistency index (k) for two alloys were discussed.

https://doi.org/10.1007/s11663-018-1372-y

I. INTRODUCTION

RHEOLOGICAL properties of semisolid slurries are the key parameter that require a further understanding for successful development of industrial semisolid forming processes and technologies due to the complex rheological phenomena during the forming process.[1–3] The rheological properties (*i.e.,* viscosity *vs* shear rate) of the semisolid slurries rely on the non-dendritic microstructure of the semisolid metallic alloys consisting of solid globular grains in a liquid matrix.[4] The viscosity of the semisolid slurry drops under shearing, and the slurry flows. The semisolid slurry can stand its own weight when allowed.[5] In the practice, the semisolid forming of aluminum alloys takes place in a fraction of a second.[6] Thus, the transient rheological behavior governs the flow behavior of the semisolid slurry within the die cavity during the semisolid forming process.[7] On the other hand, it is widely reported that the viscosity strongly depends on the solid content of the semisolid slurry and the process temperature,[7–9] in which 1 K variation in temperature can have a substantial influence on the viscosity.[8] This implies that the semisolid slurry will experience a significant variation in the viscosity during the die filling due to the rapid heat loss of the slurry in the contact with the die. The issue can be very critical for the semisolid forming of high-strength wrought aluminum alloys such as 7xxx series,[10] in which there are sharp changes in the solid content of the semisolid slurry as a function of the semisolid temperature.[11] This can cause on the one hand several manufacturing defects such as incomplete die filling that requires an extensive die modification and process optimization.[12] On the other hand, the precise modeling and simulation of the flow behavior of the slurry within the die will become very complex.[13,14] In order to minimize the complexity of the transient rheological behavior of the semisolid slurries, the transient rheological behavior of the semisolid slurries needs to become less sensitive to the solid content of the semisolid slurries. A significant improvement in the semisolid forming process can be achieved by using the semisolid slurry feedstock showing consistent transient rheological properties within a wide range of solid contents. A detailed study is required to understand the dependency of the transient rheological behavior of the semisolid slurries to the solid contents and the microstructural characteristics such as grain size and morphology of the slurries.[15]

AMIR BOLOURI is with the Department of Engineering Design and Mathematics, University of the West of England, Coldharbour Lane, Bristol BS16 1QY, UK. Contact e-mail: amir.bolouri@uwe.ac.uk X.-GRANT CHEN is with the Department of Applied Science, University of Quebec at Chicoutimi, Saguenay, QC G7H 2B1, Canada.

Manuscript submitted May 10, 2018.
Article published online August 1, 2018.

There have been several publications on the use of different methods to study the rheological behavior of the semisolid slurries.[16–19] However, there are a few successful methods and publications on the examination of the transient rheological behavior under the rapid shear rate changes. For instance, although the semisolid back extrusion process has been used,[20] it has been concluded that the process is not suitable for characterizing the rheological properties of semisolid slurries with high solid contents due to the liquid segregation.[16] Furthermore, the rheological measurement of the rapid shear change is beyond the capacity of the conventional rotational rheometers.[6,7] Rapid parallel plate compression tests have been successfully employed by Kapranos,[17] Liu,[18] Yurko,[8] and recently by Hu[21] to examine the transient rheological behavior of semisolid alloys with high solid contents. Based on these studies, some viscosity models have been proposed to include the parameters affecting the rheological properties of the semisolid slurries.[13,21,22] Nevertheless, the samples tested in these studies are not comparable in size with the semisolid bulk slurry feedstock used in the practical semisolid forming. This introduces major errors in simulating the semisolid forming process because the transient rheological behavior of the semisolid bulk slurry significantly varies from its center to the surface.[6] Nafisi *et al*.[19,23] studied the rheological properties of the semisolid bulk slurries with different solid contents and microstructural features by using parallel plate compression. Nonetheless, the main focus of their studies was on the steady-state rheological behavior under the low constant shear rates and excluded the transient rheological behavior. The rapid compression tests on the bulk semisolid slurries can imitate the transient flow behavior of the slurries during the practical semisolid forming process. Therefore, it is essential to provide the knowledge that will help to better understand and predict the flow behavior of the semisolid slurry within the die cavity.

In the present study, the SEED (Swirled Enthalpy Equilibration Device) process is used to prepare the semisolid bulk slurries. The process involves cooling of the liquid metal while it is stirred to create a mixture of globular solid grains in a liquid matrix.[24] The SEED process is one of the few commercially available routes to prepare the semisolid bulk slurries for practical semisolid forming processes.[25] The rapid compression test is used to study the transient rheological properties of the semisolid bulk 7075 aluminum slurries with different solid contents and microstructural characteristics.

II. EXPERIMENTAL PROCEDURE

The alloy used in this study was 7075 aluminum alloy with the following chemical composition (wt pct): Zn 5.7, Mg 3.0, Cu 1.6, Si 0.4, Mn 0.3, and Fe 0.4. The liquid alloy was prepared in an electrical resistance furnace. Two sets of liquid 7075 alloys were prepared: (1) 7075 base alloy and (2) 7075-0.03 pct Ti grain-refined by the addition of 0.03 pct Ti *via* an Al-5 pct Ti-1 pct B master alloy to the liquid 7075 alloy to achieve the grain morphology modification.

The SEED process was used to prepare the semisolid bulk slurries. Full details of SEED process can be found elsewhere.[24,26] The liquid alloy was ladled into a metallic mold and the mechanical stirring (swirling) was applied at 180 RPM.[27] The pouring temperature was set at 1023 K (750 °C). The mold was a BN_2-coated steel mold with a thickness of 1.5 mm, preheated at 373 K (100 °C). The dimensions of the semisolid slurries were 90 mm in diameter and 150 mm in height. The temperatures of the semisolid slurries were continuously monitored at the mid-point (the point between the center and the surface of the slurry) and at the lateral surface of the semisolid slurries. The temperature difference between these two points was less than 1 K for all the experiments. The reported temperatures correspond to the temperature reading from the mid-point. When the predetermined temperatures were achieved, swirling was stopped, and the semisolid slurry was demolded for water quenching or transferred to the rapid compression testing machine. The processing temperatures and the corresponding solid contents were determined for the experiment alloy based on differential scanning calorimeter studies conducted by our previous work published elsewhere.[27] All tests were conducted at the temperatures between 883 K and 895 K (610 °C and 622 °C) corresponding to the solid contents of 0.60 to 0.42.

The transient rheological properties of the semisolid slurries with different solid contents were evaluated by using a parallel plate rapid compression testing machine.[28] The semisolid slurries were quickly transformed into the cavity where the parallel plates were located and the rapid compression testing took place. The temperature of the cavity and the parallel plates was set the same as the predetermined processing temperature. Immediately, the upper plate with a weight of 36 kg was released under the gravity and the semisolid slurry was rapidly compressed by the upper plate movement. A precise displacement transducer (0 to 255 mm) was used to monitor the movement of the upper plate as a function of time.

III. RESULTS AND DISCUSSION

A. *Effect of SEED and Grain Refiner on Microstructures of 7075 Alloy*

Figure 1 demonstrates typical as-cast microstructures for the unprocessed 7075 alloy, SEED-processed 7075 base, and 7075-0.03 pct Ti alloys at different processing temperatures (solid contents). For the unprocessed alloy, the liquid 7075 aluminum billet was cooled down to 889 K (616 °C) by natural air cooling, and subsequently, the billet was water-quenched. The as-cast microstructure of the unprocessed alloy consists of large dendritic grains with the average grain size of 125 ± 15 μm (Figure 1(a)). In comparison with the unprocessed 7075 alloy, the microstructures of the

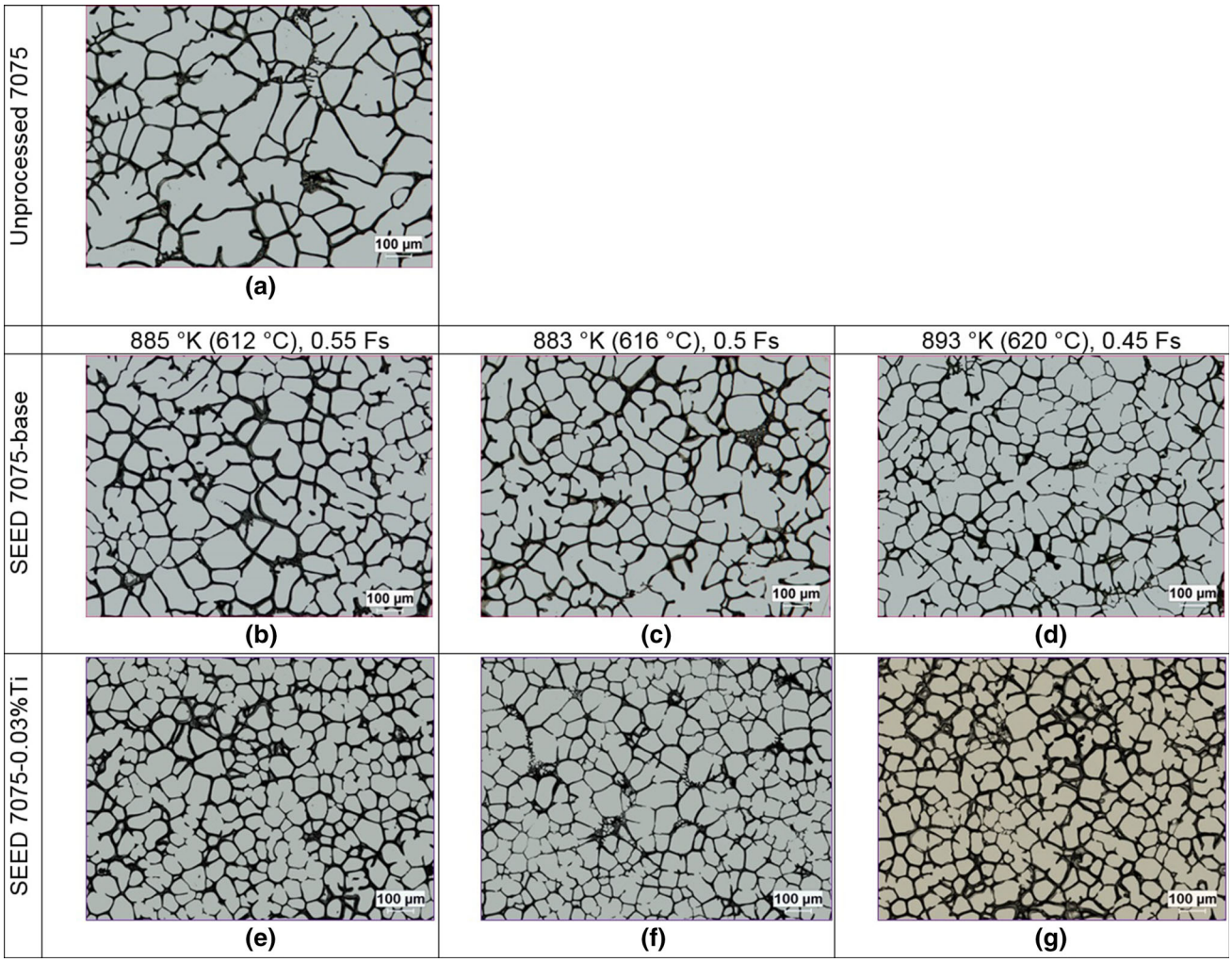

Fig. 1—As-cast microstructures of (*a*) unprocessed 7075, (*b* through *d*) SEED-Processed 7075 base and (*e* through *g*) SEED-Processed 7075-0.03 pct Ti billets at different processing temperatures.

SEED-processed 7075 base alloy comprise smaller rosette-like α-Al grains (Figure 1(b) through (d)). For the 7075 base alloy, the increase in the solid content from 0.45 to 0.55 leads to the increase in the average grain size from 104 ± 11 to 112 ± 15 μm, while their aspect ratios slightly improve from 1.7 to 1.65. Clearly the swirling (stirring effect) results in breaking the dendritic arms, leading to finer grains with improved globularity.[25,29] The addition of TiB_2 grain refiner modifies the microstructures of the SEED-processed 7075-0.03 pct Ti alloy.[30] Therefore, the α-Al grains appear smaller and evidently more globular compared to 7075 base alloy (Figures 1(e) through (g)). For 7075-0.03 pct Ti alloy, in the case of 0.45 to 0.55 solid contents, the average grain size slightly increases from 94 ± 7 to 96 ± 9 μm. Furthermore, compared to the 7075 base alloy, the aspect ratio values are considerably smaller in the range of 1.59 to 1.56 (more globular grains) for the SEED-processed 7075-0.03 pct Ti alloy with the solid contents between 0.45 and 0.55. The main reason for the modification in the microstructural features of 7075-0.03 pct Ti is due to the effect of Al5Ti1B grain refiner that the solidification mainly progresses through the nucleation of new grains rather than growth of the exciting grains.[31]

B. *Semisolid Deformation Behavior of 7075 Alloys*

The SEED-processed 7075 base and 7075-0.03 pct Ti semisolid billets with different solid contents were deformed in the rapid compression test under a constant force. Figure 2 compares the compressed billets at different processing temperatures (solid contents) for both alloys. A full deformation takes place for 7075-0.03 pct Ti billets at a wide temperature range of 885 K to 895 K (612 °C to 622 °C) and a solid content of 0.4 to 0.6 Fs, while it is very limited for 7075 base billets, for which that a considerable deformation only occurs for the temperature range of 891 K to 895 K (618 °C to 622 °C) and 0.4 to 0.46 Fs. The semisolid slurries of 7075 base alloy are hardly deformed below 891 K (618 °C) (solid contents higher than 0.46). This

clearly reflects the effect of the semisolid microstructure (*e.g.*, grain morphology and size) on the deformation behavior for semisolid 7075 wrought alloy.

Figure 3 shows the deformed curves of 7075 base and 7075-0.03 pct Ti semisolid billets under the rapid compression tests as a function of compression time. Normalized height reductions (h/h_0) of the semisolid billets were calculated, in which h is the reducing instantaneous height of billet and h_0 is the initial height of billet. The normalized height reduction represents the level of deformation occurred during the rapid compression: the lower h/h_0 value shows the higher level of deformation. For 7075 base alloy by increasing the solid content, the level of deformation significantly decreases (Figure 3(a)). By remarkable contrast, the level of deformation for 7075-0.03 pct Ti alloy appears to be independent from the solid content for a range of 0.42 to 0.53 solid content (Figure 3(b)). As discussed earlier in Section III–A (Figures 1(e) through (g)), within this solid content range for 7075-0.03 pct Ti alloy, there is no substantial change in the size of α-Al grains and their morphology. Therefore, it can be suggested that for 7075-0.03Ti alloy, the deformation behavior is not influenced by the increase of the solid content due to the consistency in features of α-Al grains such as their size and morphology within the range of 0.42 to 0.53

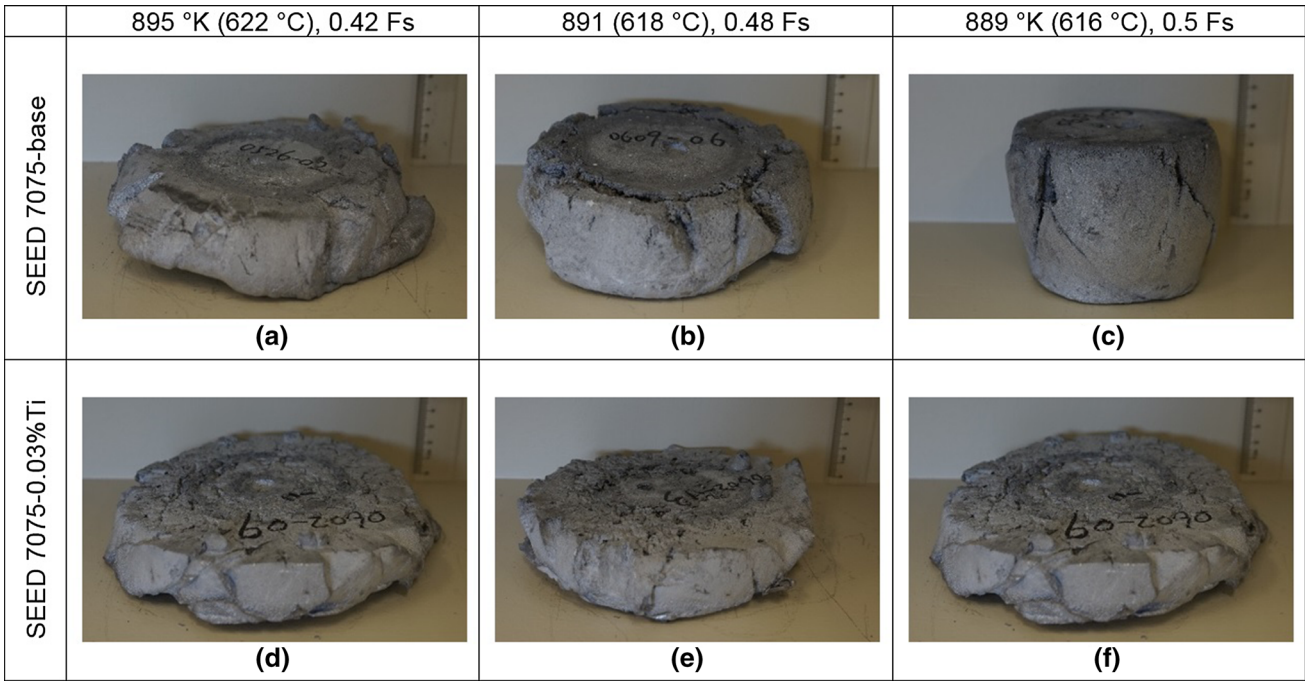

Fig. 2—Images of SEED-Processed (*a* through *c*) 7075 base and (*d* through *f*) 7075-0.03 pct Ti billets with different solid contents after deformation under the rapid compression test.[27]

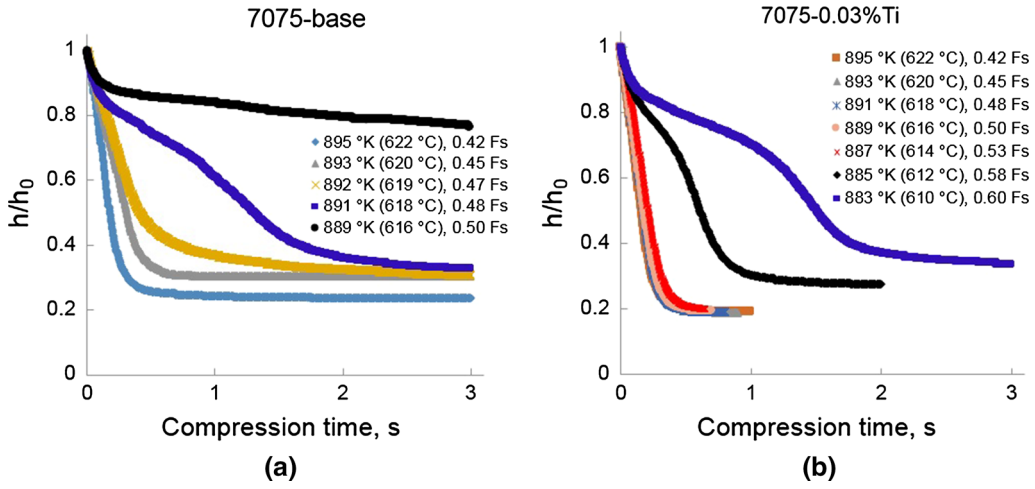

Fig. 3—Normalized height reduction (h/h_0) as a function of compression time for (*a*) 7075 base and (*b*) 7075-0.03 pct Ti semisolid billets with different solid contents.

solid content. However, by further increase in the solid content to 0.55 and 0.60 for 7075-0.03 pct Ti alloy, the effect of the solid content on the deformation becomes evident and there is clear resistance to the deformation by the billet under the constant deforming force. It is worth mentioning that increasing the solid content from 0.53 to 0.60 results in a considerable increase of the grain size from 96 ± 9 to 107 ± 11 μm.

In practical semisolid forming processes, the die filling process takes places in less than one second.[9] In other words, a large amount of deformation will occur in a very short time. Therefore, for this study, semisolid billets with a limited level of deformation in the rapid compression test are not considered for further discussion. For the rest of this study, results are shown and discussed for 7075 base billets in the range of 892 K to 895 K (619 °C to 622 °C) (Fs = 0.47 to 0.42) and for 7075-0.03 pct Ti billets in the range of 887 K to 895 K (614 °C to 622 °C) (Fs = 0.53 to 0.42).

C. *Rheological Analysis of Semisolid 7075 Alloys*

In order to calculate the average shear rate and the viscosity of the semisolid alloys, the equations proposed by Yurko and Flemings[8] for the rapid compression test were used. Equation [1] was used to calculate the average shear rate. The viscosity was calculated using Eq. [2]:

$$\dot{\gamma} = \frac{R}{2h^2}\frac{\mathrm{d}h}{\mathrm{d}t} \qquad [1]$$

$$F = \frac{-3\mu v^2}{2\pi h^5}\left(\frac{\mathrm{d}h}{\mathrm{d}t}\right), \qquad [2]$$

where $\dot{\gamma}$ is the shear rate, R is the instantaneous radius of the billet, h is the instantaneous height of billet, t is the time, F is the applied force, μ is the apparent viscosity, and v is the volume of the semisolid billet. All compression tests were conducted under a dead weight of 36 kg applying approximately a constant force of 350 N. According to data provided in Figure 3, $\mathrm{d}h/\mathrm{d}t$ values as a function of the compression time were calculated for both alloys and were used for rheological analysis in the rapid compression test.

The average shear rates as a function of the compression time are shown in Figure 4. It can be seen that the shear rate increases to a maximum value and then decreases to a very small value. The sharp increase in the shear rate can be attributed to the de-agglomeration of the grains in the semisolid billets.[32] Initially, the α-Al grains in the as-cast microstructures (Figure 1) appear to be more or less inter-locked and agglomerated through arms. However, the arms are bent during the compression and they might be broken. Therefore, due to the fast de-agglomeration and breakdown of weakly agglomerated grains, the semisolid slurry experiences an increased shear rate during the deformation under a constant force. Figures 5 and 6 show the microstructures of the alloys after the deformation (deformed billets) under the rapid compression test. In comparison with the as-cast billets in Figure 1, the α-Al grains appear finer and more globular in the microstructures of the deformed billets that support the discussion on the de-agglomeration of the grains during the deformation and rapid compression. A maximum degree of the de-agglomeration can be assumed at the maximum shear rate.

Furthermore, under the identical compression condition, 7075 base alloy experiences remarkably lower shear rates compared to 7075-0.03 pct Ti. This can be linked to the distinct microstructural features for both alloys. Due to the microstructural differences for both alloys, the motion of the α-Al grains within the semisolid slurries will be different.[15] For example, compared to the 7075 base alloy, within 7075-0.03 pct Ti semisolid slurries, the α-Al grains appear more globular and smaller, which can result in smaller contact points among the grains when the grains move along each other. Consequently, for 7075-0.03 pct Ti slurries, the grains can move and slide faster among each other during the compression. In other words, the α-Al grains with smaller size and more globular morphology within semisolid 7075-0.03 pct Ti slurries move and rotate faster to accommodate the applied shear and deformation. Therefore, under the identical compression deformation, 7075-0.03 pct Ti slurry can be sheared faster compared to the 7075 base slurry that results in considerably higher shear rates.

The apparent viscosity as a function of time is calculated and shown in Figure 7. For the sake of clear comparison, the results are shown in the logarithmic scale. In general, 7075 base alloy shows higher viscosity values compared to 7075-0.03 pct Ti alloy. The apparent viscosity is a measure of frictional forces arising from moving α-Al grains alongside each other within the semisolid structure.[33] There could be several interactions among the grains and between the grains and the liquid matrix,[19] which will influence the apparent viscosity of the semisolid alloys. Due to the large and irregular inter-connected α-Al grains within the microstructure of 7075 base semisolid slurries, they are not able to easily slide or rotate when the shearing is applied. This raises the frictional forces within 7075 base alloy semisolid microstructure that leads to significantly higher viscosity values compared to 7075-0.03 pct Ti alloy with globular and fine α-Al grains that can easily slide alongside each other.

For the 7075 base alloy, the viscosity exhibits evident dependency on the solid content. On the contrary, for 7075-0.03 pct Ti, there is very little dependency on the solid content for the range of 0.45 to 0.50 solid content. It seems that the viscosity of semisolid aluminum alloys can become independent from the solid content for a specific range. This is against the general belief that the viscosity strongly depends on the solid content.[7] This can be explained as that for most of the literature, there is a significant growth in grain size simultaneously with the increase in the solid content as it is for the 7075 base alloy in this study. Therefore, the viscosity is significantly influenced by increasing the solid content because it becomes difficult for the larger grains to move

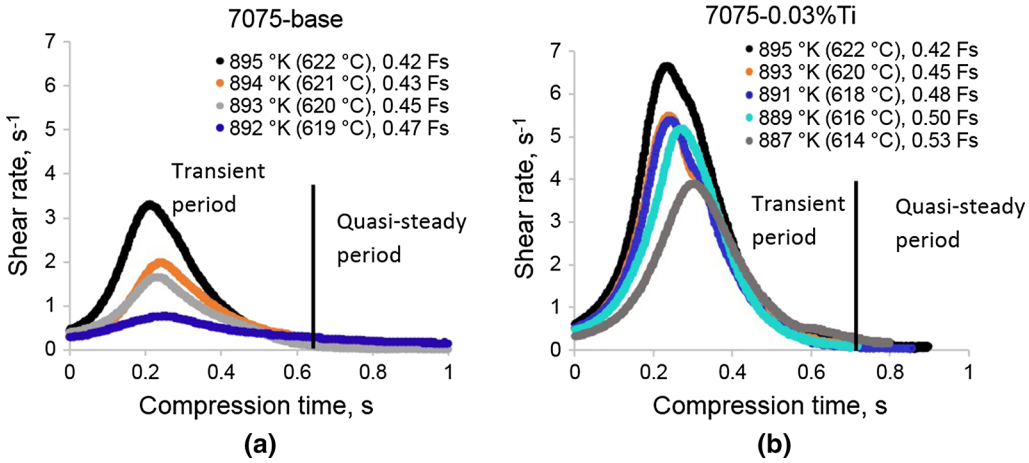

Fig. 4—Shear rate as a function of compression time for (*a*) 7075 base and (*b*) 7075-0.03 pct Ti billets with different solid contents.

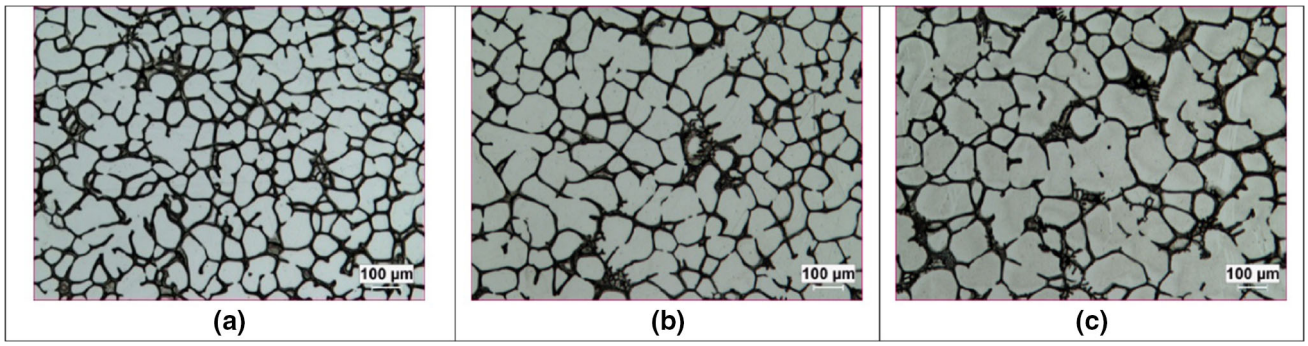

Fig. 5—Microstructures of deformed billets for 7075 base alloy with (*a*) 895 K (622 °C) 0.42 Fs, (*b*) 893 K (620 °C) 0.45 Fs and (*c*) 891 K (618 °C) 0.48 Fs.

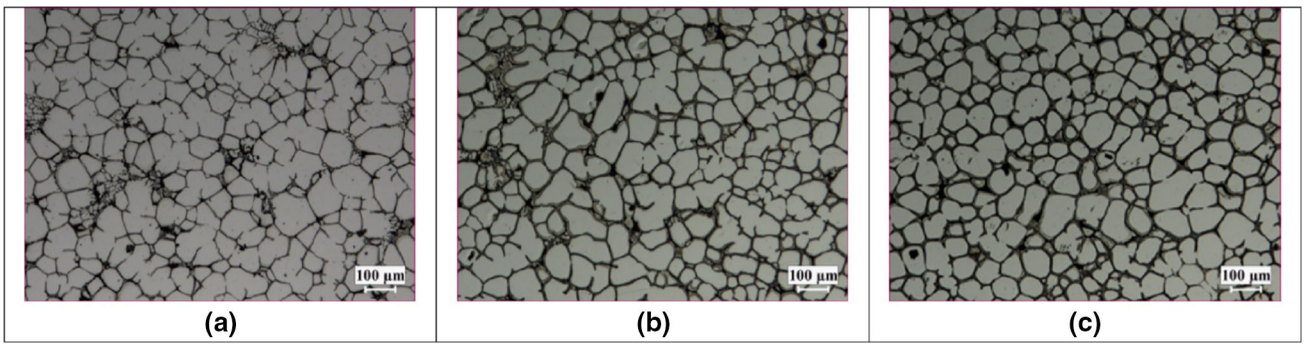

Fig. 6—Microstructures of deformed billets for 7075-0.03 pct TiB_2 alloy at (*a*) 895 K (622 °C) 0.42 Fs, (*b*) 889 K (616 °C) 0.50 Fs, and (*c*) 887 K (614 °C) 0.53 Fs.

alongside each other and the frictional force increases resulting in a high viscosity. However, for 7075-0.03 pct Ti alloy, due to the microstructural modification, the grain size remains in a constant range despite an increase in the content solid range of 0.45 to 0.50, and the viscosity is not dominantly influenced as a result of the increase in the solid content.

D. *Viscosity vs Shear Rate Under Transient State*

In the present study, a constant shear rate was unlikely to occur during rapid compression. However, a quasi-steady period can be assumed, when the change in the shear rate is small for a considerable period of compression. Accordingly, the transient state was considered just before the quasi-steady state as shown in Figure 4.

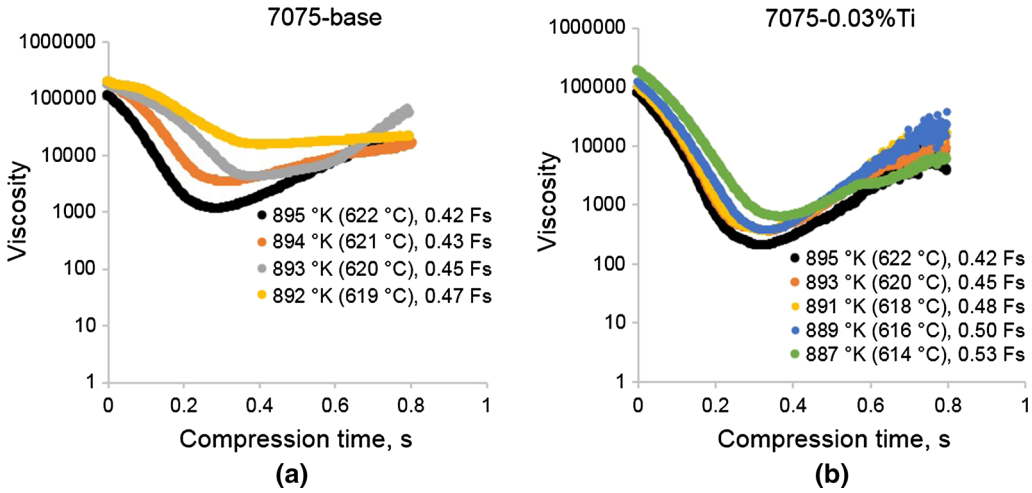

Fig. 7—Viscosity as a function of compression time for (*a*) 7075 base and (*b*) 7075-0.03 pct Ti billets with different solid contents.

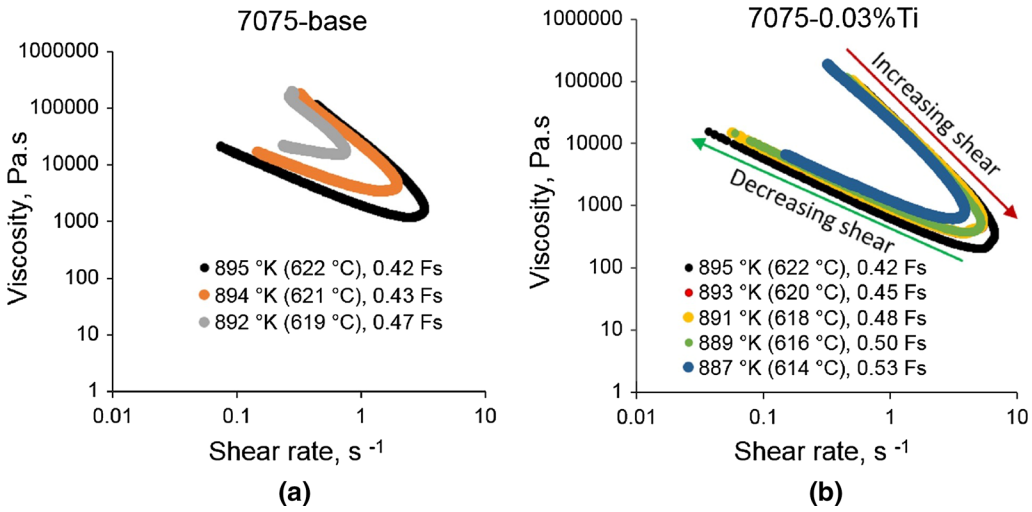

Fig. 8—Shear rate–viscosity correlation for (*a*) 7075 base and (*b*) 7075-0.03 pct Ti billets with different solid contents.

Figure 8 shows the viscosity *vs* the shear rate for the alloys with different solid contents. The graphs clearly exhibit increasing and decreasing shear rate periods. The viscosity behaves inversely with the shear rate during compression indicating a shear-thinning manner.[34] In other words, as the shear rate increases, the apparent viscosity decreases to a minimum value followed by an increase in the viscosity as shear rate decreases to a very small value. However, after the maximum shear rate, there is no substantial increase in the apparent viscosity of the billets. Thus, there are two different apparent viscosities for one identical shear rate value in the increasing and decreasing shear rates periods, in which the viscosity in the decreasing shear rate region is significantly smaller than the viscosity in the increasing share rate. It can be assumed that at the beginning of the deformation the grains are inter-locked exhibiting a high viscosity.

Subsequently, the grains and arms among them are bent during the deformation and the bonds among them are eventually broken. When the maximum de-agglomeration of grains occurs at the maximum shear rate during compression, the re-agglomeration of the grains is negligible or very slow in the decreasing shear rate period of the test because they are diffusion control processes. Therefore, there is no substantial increase in the viscosity due to the reduction in the shear rate.

For the 7075-0.03 pct Ti alloy at different solid contents, the apparent viscosity values in the decreasing or increasing shear rate periods are not substantially influenced by the solid content. In other words, considerable differences between the apparent viscosity values are not evident in the labeled increasing or decreasing shear rate periods for the semisolid billets with different solid contents. The consistent rheological behavior in the increasing shear rate period is due to the consistent

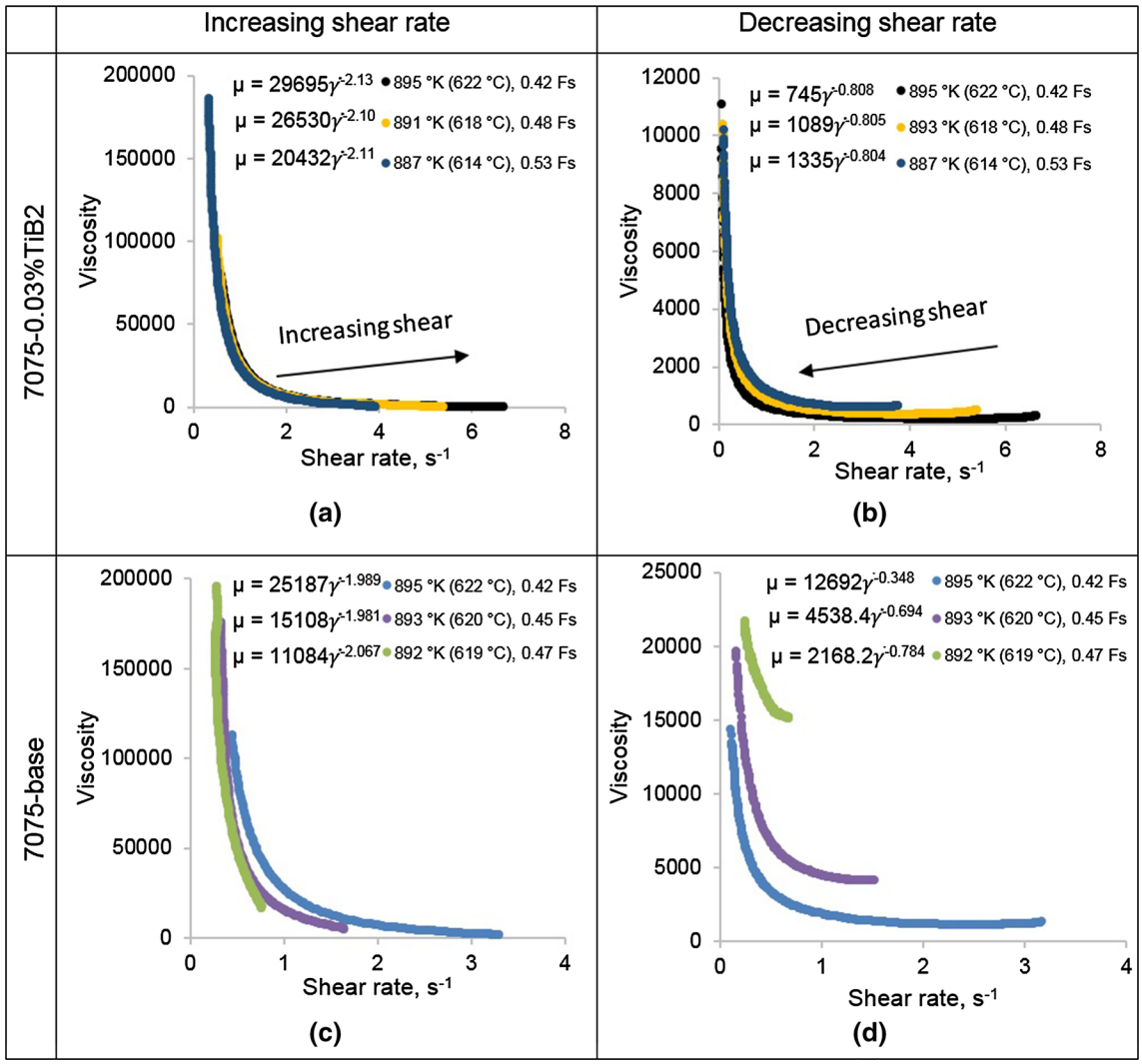

Fig. 9—Fitted power law equation for (*a*, *b*) 7075-0.03 pct Ti and (*c*, *d*) 7075 base semisolid billets in the increasing and decreasing shear rate periods.

initial as-cast microstructures of the billets as discussed in Section I. In addition, the small change in the rheological properties in the decreasing share rate period can be explained according to the deformed microstructures in Figure 5. Despite the substantial change in the solid content, there is a very limited effect on the features of globular α-Al grains in the microstructures of the deformed billets and the microstructures consist of small globular grains. On the contrary, as can be seen in Figure 4 for the 7075 base alloy, by increasing the solid content, the size of the α-Al grains appears larger, thereby explaining the significant difference in the rheological properties in the decreasing shear rate period.

In the practical process of semisolid high-pressure die casting, the increasing shear rate periods correspond to when the semisolid slurry just enters into the runner of the die and the maximum shear rates are easy to occur during this process.[21] The viscosity values in the decreasing shear rate periods correspond with the die filling period, and therefore, they are remarkably important to analyzing the die filling behavior of the semisolid slurry.

One of the important issues during die filling process in the semisolid high-pressure die casting is the change of the solid content of the semisolid slurry due to its contact to a relatively cold die and the consequent temperature loss as the filling progresses, which implies a significant change in the viscosity of the semisolid slurry.[7] However, as a result of microstructural modification to 7075-0.03 pct Ti semisolid slurries, very minimal changes in the apparent viscosity of the semisolid slurries occurred at a certain range of solid contents in the decreasing shear periods (die filling period). Consequently, in the semisolid high-pressure die casting process, the die can be perfectly filled with the slurry possessing a less sensitive viscosity to the solid content. Thus, it can provide more controlled and predictable die filling behavior and manufacturing process. By remarkable contrast, for the 7075 base

alloy, there was a large difference in the apparent viscosity in the shear rate decreasing period for the slurries with slightly different solid contents. Therefore, as discussed earlier due to the change of the solid content of the semisolid slurry during die filling process, on the one hand, it can give rise to inconsistent die filling behavior and the quality of components,[22] and on the other hand, it can make the temperature control a central issue during the process.[7] In addition, this will make the researcher unable to properly adopt a model for the predication of the flow behavior of the semisolid slurries.[6]

E. *Power Law Viscosity Model*

The power law viscosity model, $\mu = k\dot{\gamma}^{-n}$, has been widely used to study viscosity change as a function of applied shear rate for semisolid alloys, where k is the consistency index and n is the flow behavior index.[13] In this study, the decreasing and increasing shear rate periods are separately fitted to the power law model. For the 7075 base alloy, it was not possible to fit a model with the solid contents higher than 0.47 due to a very low correlation coefficient for the fitted equations. The typical results are shown in Figure 9.

In the increasing shear rate period for the 7075-0.03Ti alloy (Figure 9(a)), it appears that the flow behavior index (n) is independent to the solid content within a large window of 0.42 to 0.53 solid contents, in which n remains approximately constant around 2.1. However, for the 7075 base alloy within a narrow range of 0.42 to 0.47 solid contents (Figure 9(c)), the flow behavior index (n) shows a moderate dependency to the solid content, in which n increases from 1.98 to 2.10. On the other hand, the influence of the solid content on the consistency index (k) is very evident for 7075 base alloy, and the k considerably varies by 55 pct when the solid content changes by only 5 pct from 0.42 to 0.47. On the contrary, the variation in the k value is a very small amount for 7075-0.03Ti alloy, which is only 10 pct for the 5 pct change in the solid content.

As discussed earlier, the modeling for the flow behavior of semisolid slurries in the decreasing shear rate period is important because the die filling predominantly occurs in the shear rates and viscosities corresponding to this period.[21] In the decreasing shear rate period for 7075-0.03 pct Ti slurries, there is an extremely small sensitivity of the flow behavior index (n) to the increasing solid content in a wide range of 0.42 to 0.53, in which n can be assumed to be constant at 0.805. On the contrary, in the decreasing shear rate period for 7075 base alloy, n appears significantly sensitive to the solid content that changes from 0.784 to 0.348 by increasing the solid content from 0.42 to 0.47. Moreover, for 7075 base slurries in a narrow solid content range, the consistency index (k) sharply decreases from 12692 (at 0.42 solid content) to 2168 (at 0.47 solid content), while for 7075-0.03 pct Ti slurries in a wider solid content range, k only varies from 745 (at 0.42 solid content) to 1335 (at 0.53 solid content). Therefore, it could be concluded that compared to unrefined 7075 base semisolid alloy, the rheological behavior of 7075-0.03 pct Ti semisolid alloy can be consistently and more precisely described according to the power law. Knowing such difference caused by the α-Al grain morphology and size, it will greatly increase the predicting capacity of any simulation study on the die filling process for semisolid 7075 aluminum alloys.

IV. CONCLUSIONS

(1) Compared to the unprocessed 7075 aluminum alloy, the SEED semisolid process produced finer rosette-like α-Al grains with improved globularity. The addition of TiB_2 grain refiner further modified the grain morphology and size, resulting in a fully globular structure with smaller grain size.
(2) The 7075 base alloy exhibited a narrow window of solid contents (0.42 to 0.47 Fs), in which the semisolid slurry can be deformed. The level of deformation significantly decreases with increasing the solid content. On the contrary, the grain-refined 7075-0.03 pct Ti alloy can be easily deformed at a wider range of solid contents (0.42 to 0.53 Fs), in which the deformation level appears to be independent from the solid content.
(3) During compression deformation in the transient state, the shear rate increases to a maximum value and then decreases to a very small value in the less than one second. Under the identical condition, the 7075 base alloy experiences remarkably lower shear rates compared to the 7075-0.03 pct Ti alloy.
(4) Under the transient state, the rheological properties (*i.e.,* viscosity *vs* shear rate) of the semisolid slurries exhibit increasing and decreasing shear rate periods. The apparent viscosity of 7075 base alloy exhibits a dependency on the solid content solid. For the 7075-0.03 pct TiB_2 alloy at different solid contents, the apparent viscosity values in the decreasing or increasing shear rate periods are not substantially influenced by the solid content. It can provide more controlled and predictable die filling behavior and manufacturing process.
(5) For the 7075-0.03 pct TiB_2 semisolid slurries, the flow behavior index (n) and the consistency index (k) are less sensitive to the solid content compared to 7075 base semisolid slurries.

ACKNOWLEDGMENTS

The authors would like to acknowledge the financial support of the Natural Sciences and Engineering Research Council of Canada (NSERC) and STAS Inc. through the NSERC Industry Research Chair in the Metallurgy of Aluminum Transformation at University of Quebec at Chicoutimi. The authors would like to acknowledge the financial support of University of the West of England. The authors would also like to thank Mr. Q. Zhao for his assistance in the experiments.

REFERENCES

1. F. Czerwinski: *Metall. Mater. Trans. B*, 2017, vol. 48B, pp. 367–93.
2. H.V. Atkinson and V. Favier: *Metall. Mater. Trans. A*, 2016, vol. 47A, pp. 1740–50.
3. J. Rogal: *Mater. Sci. Technol. (United Kingdom)*, 2017, vol. 33, pp. 759–64.
4. D.B. Spencer, R. Mehrabian, and M.C. Flemings: *Metall. Trans.*, 1972, vol. 3, pp. 1925–32.
5. Z. Fan: *Int. Mater. Rev.*, 2002, vol. 47, pp. 49–85.
6. D. Kirkwood and P. Ward: *Steel Res.*, 2004, vol. 75, pp. 519–24.
7. H.V. Atkinson: *Comprehensive Materials Processing*, 1st ed., Elsevier, New York, 2014, vol. 5, pp. 149–62.
8. J.A. Yurko and M.C. Flemings: *Metall. Mater. Trans. A*, 2002, vol. 33A, pp. 2737–46.
9. T.Y. Liu, H.V. Atkinson, P. Kapranos, D.H. Kirkwood, and S.C. Hogg: *Metall. Mater. Trans. A*, 2003, vol. 34A, pp. 1545–54.
10. A. Bolouri and C.G. Kang: *Metall. Mater. Trans. A*, 2014, vol. 45A, pp. 2575–89.
11. S. Liang, R. Chena, and E. Hana: *Int. J. Mater. Res.*, 2010, vol. 101, pp. 256–64.
12. J. Rogal, H.V. Dutkiewicz, L. Atkinson, T. Lityńska-Dobrzyńska, and M. Modigell: *Mater. Sci. Eng. A*, 2013, vol. 580, pp. 362–73.
13. H.V. Atkinson: *Prog. Mater. Sci.*, 2005, vol. 50, pp. 341–412.
14. A. Neag, V. Favier, R. Bigot, and H.V. Atkinson: *J. Mater. Process. Technol.*, 2016, vol. 229, pp. 338–48.
15. S. Zabler, A. Ershov, A. Rack, F. Garcia-Moreno, T. Baumbach, and J. Banhart: *Acta Mater.*, 2013, vol. 61, pp. 1244–53.
16. T. Basner, A. Sachdev, and R. Pehlke: *Metall. Mater. Trans. A*, 2000, vol. 31A, pp. 57–62.
17. P. Kapranos, T.Y. Liu, H.V. Atkinson, and D.H. Kirkwood: *J. Mater. Process. Technol.*, 2001, vol. 111, pp. 31–6.
18. H.V. Atkinson, T.Y. Liu, P. Kapranos, D.H. Kirkwood, and S.C. Hogg: *Metall. Mater. Trans. A*, 2003, vol. 34A, pp. 1545–54.
19. S. Nafisi, O. Lashkari, R. Ghomashchi, F. Ajersch, and A. Charette: *Acta Mater.*, 2006, vol. 54, pp. 3503–11.
20. R. Meshkabadi, V. Pouyafar, A. Javdani, and G. Faraji: *Metall. Mater. Trans. A*, 2017, vol. 48A, pp. 4275–85.
21. X.G. Hu, Q. Zhu, H.V. Atkinson, H.X. Lu, F. Zhang, H.B. Dong, and Y.L. Kang: *Acta Mater.*, 2017, vol. 124, pp. 410–20.
22. M. Modigell and J. Koke: *Mech. Time Depend. Mater.*, 1999, vol. 3, pp. 15–30.
23. S. Nafisi, D. Emadi, and R. Ghomashchi: *Mater. Sci. Eng. A*, 2009, vol. 507, pp. 87–92.
24. D. Doutre, G. Hay, P. Wales, and J.-P. Gabathuler: *Can. Metall. Q.*, 2004, vol. 43, pp. 265–72.
25. P. Côté, M.E. Larouche, and X.G. Chen: *Solid State Phenom.*, 2012, vols. 192–193, pp. 373–78.
26. D. Doutre, G. Hay, P. Wales: U.S. Patent No. 6,428,636 (August 2002).
27. A. Bolouri, Q.F. Zhao, P. Côté, and X.-G. Chen: *Solid State Phenom.*, 2016, vol. 256, pp. 288–93.
28. M. Tebib, F. Ajersch, and X.G. Chen: *Solid State Phenom.*, 2013, vols. 192–193, pp. 323–28.
29. I.G. Chung, A. Bolouri, and C.G. Kang: *Int. J. Adv. Manuf. Technol.*, 2012, vol. 58, pp. 237–45.
30. A.B. Pattnaik, S. Das, B.B. Jha, and N. Prasanth: *J. Mater. Res. Technol.*, 2015, vol. 4, pp. 171–9.
31. M.A. Easton and D.H. Stjohn: *Metall. Mater. Trans. A*, 1999, vol. 30A, pp. 1613–23.
32. C.J. Quaak, M.G. Horsten, and W.H. Kool: *Mater. Sci. Eng. A*, 1994, vol. 183, pp. 247–56.
33. G.K. Sigworth: *Can. Metall. Q.*, 1996, vol. 35, pp. 101–22.
34. D.H. Kirkwood and P.J. Ward: *Mater. Lett.*, 2008, vol. 62, pp. 3981–83.